Microwave properties of *n*-type InSb in a magnetic field between 4 and 300 °K*

I. I. Eldumiati† and G. I. Haddad

Electron Physics Laboratory, Department of Electrical and Computer Engineering, The University of Michigan, Ann Arbor, Michigan 48104

(Received 28 February 1972; in final form 11 July 1972)

A two-band conduction model is used to determine the properties of shallow-type impurity semiconductors in the presence of microwave and dc magnetic fields as a function of temperature. Measurements using cavity perturbation techniques are employed to determine the properties of *n*-type InSb and theoretical and experimental results between 4 and 300 °K are compared. The hot-electron effect was found to be insignificant between 77 and 300 °K, and the scattering mechanisms are dominated by acoustic and polar modes over the same temperature range.

INTRODUCTION

Bulk *n*-type indium antimonide is finding many applications in electron devices.[1–3] A knowledge of the microwave properties of high-purity samples in the presence of a magnetic field is very important toward achieving the potentials of these devices. The properties of such samples have been investigated by many authors.[4,5] However, in all cases dc bias was applied to the samples which requires contacting the samples and causes the electrons to be heated considerably.

The object of this paper is to investigate the properties of low-impurity InSb in the presence of microwave and dc magnetic fields as a function of temperature (4.2 °K and 77–300 °K). A cavity perturbation method is used for experimental verification. The method has two basic advantages, namely, the elimination of the need to contact the samples and the ability to work at low signal levels to avoid the effect of heating the electrons.

THEORY

Two-band conduction in InSb

Due to the small effective mass and the relatively large dielectric constant of *n*-type InSb, the donor electron-wave functions overlap even at liquid-helium temperature and reasonably low concentrations. This will cause the impurity and conduction bands to merge together, an effect which has been demonstrated by many authors.[6–8] Following Conwell's analysis[9] and using an effective mass at the conduction band edge equal to 0.0133 times the free electronic mass, the impurity and conduction bands merge together at a net impurity concentration of approximately 0.92×10^{15} cm^{-3} and a concentration of at most 0.74×10^{13} cm^{-3} is required for the familiar band picture to prevail. This analysis assumes that the impurity ions are arranged on a regular uniform lattice and the atomic polyhedron surrounding each impurity ion is approximated by a sphere whose radius r_s is given by

$$\tfrac{4}{3}\pi r_s^3 = 1/N_I, \tag{1}$$

where N_I is the net impurity concentration. It is also worth noting that if randomness is taken into account, the cited number would be lower. Between these two values of concentrations the two-band conduction model, first introduced by Hung,[10] is most suited for studying the properties of these materials.

Although the purest available InSb has a concentration greater than 10^{13} cm^{-3}, energy bands can be achieved in the presence of a magnetic field. Magnetically induced banding in InSb was discussed theoretically by Yafet *et al.*[11] and investigated experimentally by many authors, among them are Keyes and Sladek,[4] Sladek,[6] Brown and Kimmit[12] and recently by Apel *et al.*[5]

In the presence of a magnetic field the motion of the impurity electrons become quantized in the direction perpendicular to the magnetic field. The conduction band will be split into Landau levels with an energy difference of $\hbar\omega_c$, where ω_c is the angular cyclotron frequency and $\hbar$ is Planck's constant. However, it was shown by Putley[13] that the number of states in the lowest Landau level is greater than the number of available electrons for all impurity concentrations of interest. The quantization in the plane normal to the magnetic field tends to cause the electrons to become strongly tied to their impurity ions as the magnetic field is increased. At a certain value of the magnetic field B_F, essentially all the carriers become bound to their impurity ions and the overlap between the impurity and conduction bands is reduced to a minimum. The criterion for band formation is that the average cyclotron radius $\langle r_c\rangle$ equals the occupancy radius of the donor ions r_s. Assuming a hydrogenic model, the cyclotron radius corresponding to a magnetic field intensity B is given by

$$r_c = m^*v/qB, \tag{2}$$

where v is the velocity of the charge carriers in the plane perpendicular to B, and q is the carrier charge.

As a first-order approximation for determining $\langle r_c\rangle$, a Maxwellian distribution is assumed. The energy of the carriers will be given by

$$\mathcal{E} \approx kT_e + hf_{I0}, \tag{3}$$

where T_e is the electron temperature, which might be different from the lattice temperature as a result of the heating effect of the monitoring microwave radiation whose frequency is f_{I0}. At 10 GHz, hf_{I0} corresponds to 4.135×10^{-2} meV, which is too small compared to the thermal energy, down to liquid-helium temperature. Therefore, hf_{I0} can be safely neglected in Eq. (3). In addition, hf_{I0} is smaller than the $\hbar\omega_c$ values of interest, which implies that the carriers will only be limited to the first Landau level.

From Eq. (2)

$$\langle r_c\rangle = (m^*/qB)\langle v\rangle,$$

and the freeze-out magnetic field B_F can be obtained by equating r_s, defined in Eq. (1), to $\langle r_c\rangle$ giving

$$B_F = \frac{m^*\langle v\rangle}{q}\left(\frac{4\pi N_I}{3}\right)^{1/3}. \tag{4}$$

If the magnetic field is oriented along the z axis, the

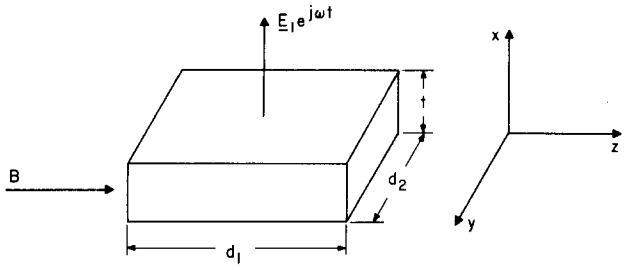

FIG. 1. Orientation of the fields applied to the bulk semiconductor.

average value of v will be given by

$$\langle v\rangle = \int_{-\infty}^{\infty} \exp(-a^2 v_z^2)\, dv_z\, 2\pi \int_0^{\infty} v^2 \exp(-a^2 v^2)\, dv \times \{\int_{-\infty}^{\infty} \exp[-a^2(v_x^2+v_y^2+v_z^2)]dv_x dv_y dv_z\}^{-1}, \quad (5)$$

where $v^2 = v_x^2 + v_y^2$ and $a^2 = m^*/2kT_e$. Carrying out the integration and substituting the value of $\langle v\rangle$ in Eq. (4) yields

$$B_F = \left(\frac{4\pi N_I}{3}\right)^{1/3} \left(\frac{\pi m^* kT_e}{2q^2}\right)^{1/2}. \quad (6)$$

The value of q will depend on the nature of the chemical bond between the indium and antimony atoms,[14,15] and can be expressed by the following relation:

$$q = ee^*, \quad (7)$$

where e^* is the effective charge ratio of the carriers. It was indicated by Cochran[16] that the effective ionic charge depends on the difference between the electronic polarizabilities of the two ions concerned and the parameters describing the short-range interaction. This idea was pursued by Hass and Henvis[17] by studying the infrared lattice reflectivity of InSb at liquid-helium temperature. Expressions for the polarizability derived by Born and Huang[18] which assume a tetrahedral symmetry were used and resulted in a value of 0.42 for e^* in the case of InSb. This value agrees fairly well with the 0.45 value obtained by x-ray diffraction.[19]

It should be noted that the values obtained from Eq. (6) are expected to be on the lower side, since 46% of the carriers have velocities larger than $\langle v\rangle$, and in turn will have a larger cyclotron radius. The magnetic field B_{Fh} required to cause 90% of the impurity electrons to have an r_c smaller than or equal to r_s is 1.72 B_F.

Conductivity of semiconductor material in crossed dc magnetic and microwave fields

This section deals with the dependence of the material conductivity and dielectric constant on crossed electric and magnetic fields whose orientation is shown in Fig. 1. Both carriers in the conduction and impurity bands contribute to these parameters. Therefore,

$$\sigma = q(\mu_c n_c + \mu_i n_i), \quad (8)$$

where μ_c and n_c are the mobility and carrier density in the conduction band, respectively, and μ_i and n_i are those in the impurity band. n_c and n_i are related to the net carrier concentration as follows:

$$n_c + n_i = N_I, \quad (9)$$

and the division of the carriers between the two bands will depend on the values of the electric and magnetic fields as well as the temperature. It is adequate to study the contribution of either kind of carrier to the conductivity and then combine the effect of both of them using Eq. (8). Begin by writing the equation of motion for the carriers in the presence of a steady magnetic induction **B** and a microwave field **E** which is expressed as

$$q\mathbf{E} + q\mathbf{v}\times\mathbf{B} = m^*\frac{d\mathbf{v}}{dt} + \frac{m^*}{\tau}\mathbf{v}, \quad (10)$$

where **v** is the average particle velocity and τ is the carrier relaxation time.

For a quasisteady state

$$\mathbf{E} = \mathbf{E}_1 \exp(j\omega t) \quad (11)$$

and

$$\mathbf{v} = \mathbf{v}_1 \exp(j\omega t). \quad (12)$$

Substituting Eqs. (11) and (12) into Eq. (10) results in

$$q\mathbf{E}_1 + q\mathbf{v}_1\times\mathbf{B} = (m^*/\tau)(1+j\omega\tau)\mathbf{v}_1. \quad (13)$$

Assuming B to be along the z axis and n to be the number of carriers per unit volume in the band under consideration, then **J**, the contribution of this band to the current density, is given by

$$\mathbf{J} = nq\mathbf{v}. \quad (14)$$

Substituting from Eq. (13) into Eq. (14) and arranging terms gives the following expression for the complex conductivity σ_c:

$$\boldsymbol{\sigma}_c = qn\mu_\omega \begin{bmatrix} \frac{1}{1+\mu_\omega^2 B^2} & \frac{\mu_\omega B}{1+\mu_\omega^2 B^2} & 0 \\ -\frac{\mu_\omega B}{1+\mu_\omega^2 B^2} & \frac{1}{1+\mu_\omega^2 B^2} & 0 \\ 0 & 0 & 1 \end{bmatrix}, \quad (15)$$

where

$$\mu_\omega = \mu_0/(1+j\omega\tau), \quad \mu_0 = (q/m^*)\tau.$$

The real part of σ_c will contribute to the conduction process within the bulk material and will be denoted by σ, while the imaginary part will be responsible for the change in the material dielectric constant. The material conductivity and relative dielectric constant are therefore given by

$$\sigma = \mathrm{Re}(\sigma_c)$$

and

$$\epsilon_r = \epsilon_l + \mathrm{Im}(\sigma_c)/)\omega\kappa_0), \quad (16)$$

where κ_0 is the permittivity of free space and ϵ_l is the lattice dielectric constant of the material.

Since InSb is isotropic, the functional dependence of the conductivity and dielectric constant can be written by substituting from Eq. (15) into Eq. (8) which yields

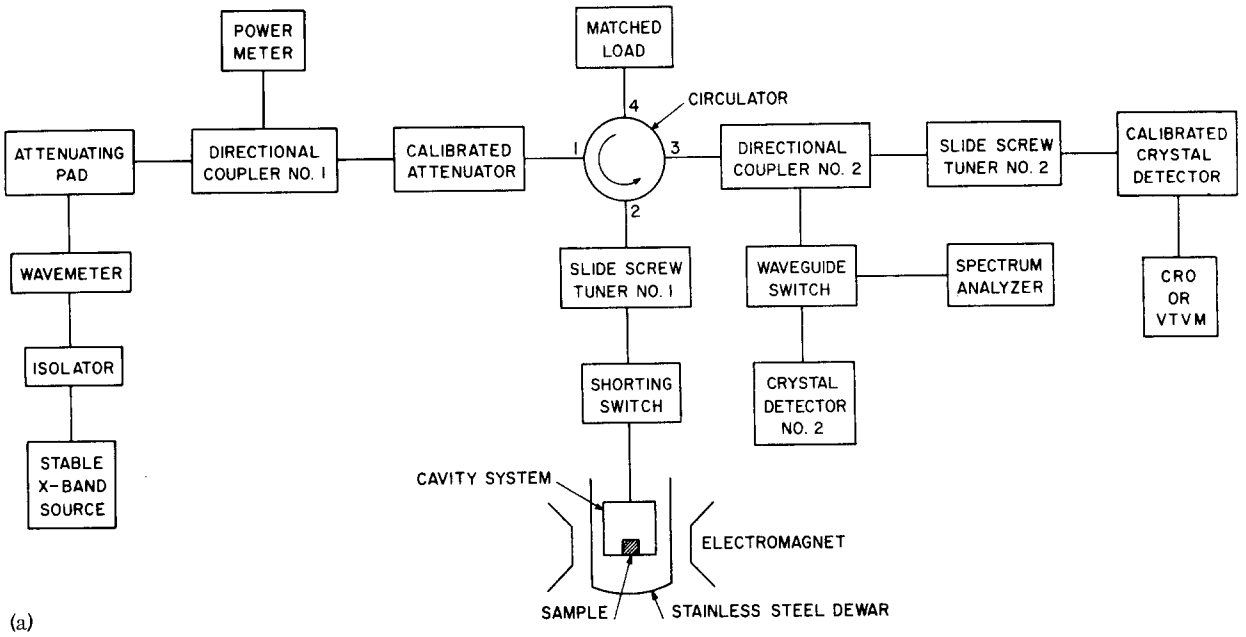

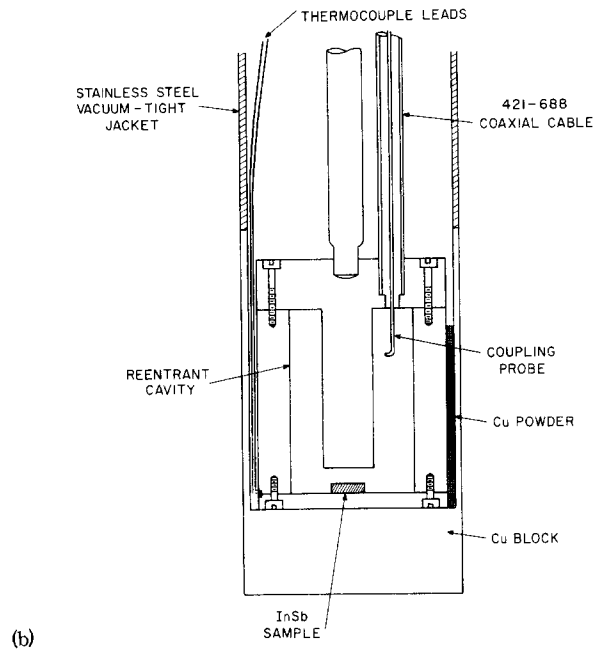

FIG. 2. (a) Microwave circuit for investigation of the material properties. (b) Cavity system for testing the material properties.

$$\sigma = q\left(n_c\mu_{c0}\frac{1+\mu_{c0}^2B^2+\omega^2\tau_c^2}{(1+\mu_{c0}^2B^2-\omega^2\tau_c^2)^2+4\omega^2\tau^2} + n_i\mu_{i0}\frac{1+\mu_{i0}^2B^2+\omega^2\tau_i^2}{(1+\mu_i^2B^2-\omega^2\tau_i^2)^2+4\omega^2\tau_i^2}\right), \tag{17}$$

and

$$\epsilon_r = \epsilon_l + \frac{q^2}{\omega^2K_0}\left(\frac{n_c}{m_c^*}\frac{(\mu_{c0}^2B^2-\omega^2\tau_c^2-1)\omega^2\tau_c^2}{(1+\mu_{c0}^2B^2-\omega^2\tau_c^2)^2+4\omega^2\tau_c^2} + \frac{n_i}{m_i^*}\frac{(\mu_{i0}^2B^2-\omega^2\tau_i^2-1)\omega^2\tau_i^2}{(1+\mu_{i0}^2B^2-\omega^2\tau_i^2)^2+4\omega^2\tau_i^2}\right), \tag{18}$$

where μ_{c0} and μ_{i0} are the dc mobilities in the conduction and impurity bands, respectively. In order to determine the dependence of n_c and n_i on the magnetic field, the cyclotron radius of the individual carriers is compared with r_s. A carrier will belong to the conduction band if r_c is greater than r_s, and to the impurity band if the opposite is true. The average speed v_0 at which the cyclotron radius equals the occupancy radius r_s is given by

$$v_0 = (qr_s/m^*)B\,.$$

Substituting the value of r_s as defined in Eq. (1) yields[20]

$$v_0 = \frac{q}{m^*}\left(\frac{3}{4\pi N_I}\right)^{1/3}B. \tag{19}$$

Those electrons whose speed in the plane normal to B is greater than v_0 will belong to the conduction band, while the rest will be in the impurity band. Among N_I particles having a Maxwellian distribution and an effective temperature T_e, the number of particles n'_{v_0} whose speed in an arbitrary plane is greater than v_0 is given by

$$n'_{v_0} = N_I\exp(-m^*v_0^2/2kT_e). \tag{20}$$

Combining Eqs. (20), (19), and (9) yields

$$n_c = N_I\exp(-bB^2) \tag{21}$$

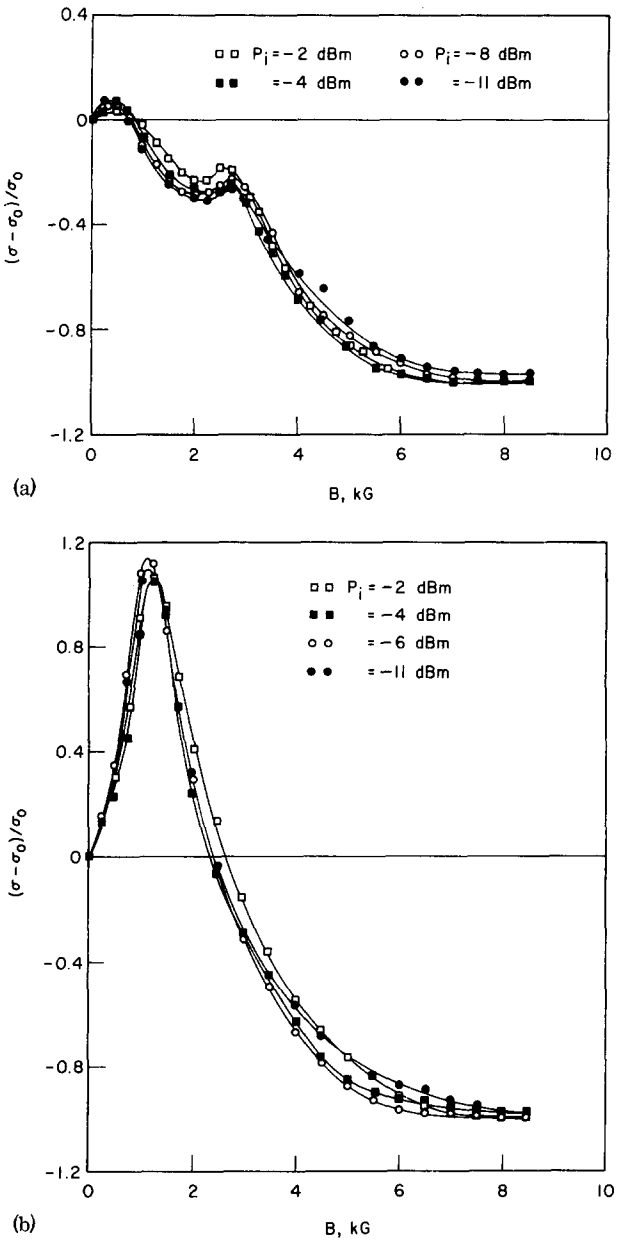

FIG. 3. $(\sigma-\sigma_0)/\sigma_0$ vs B at 77°K. (a) B is normal to the (110)-crystal plane. (b) B is parallel to the (110)-crystal plane.

and

$$n_i = N_I[1-\exp(-bB^2)], \tag{22}$$

where

$$b=\frac{q^2}{2m^* kT_e}\left(\frac{3}{4\pi N_I}\right)^{2/3}. \tag{23}$$

Substituting the values of n_c and n_i, as obtained in Eqs. (20) and (21), into Eqs. (17) and (18) yields the following expressions for ϵ_r and σ:

$$\sigma = qN_I\left(\mu_{co}\frac{1+\mu_{co}^2B^2+\omega^2\tau_c^2}{(1+\mu_{co}^2B^2-\omega^2\tau_c^2)^2+4\omega^2\tau^2}\exp(-bB^2)\right.$$

$$\left.+\mu_{io}\frac{1+\mu_{io}^2B^2+\omega^2\tau_i^2}{(1+\mu_{io}^2B^2-\omega^2\tau_i^2)^2+4\omega^2\tau_i^2}[1-\exp(-bB^2)]\right), \tag{24}$$

and

$$\epsilon_r=\epsilon_l+\frac{qN_I}{\omega^2\kappa_0}\left(\frac{1}{m_c^*}\frac{(\mu_{co}^2B^2-\omega^2\tau_c^2-1)\omega^2\tau_c^2}{(1+\mu_{co}^2B^2-\omega^2\tau_c^2)^2+4\omega^2\tau_c^2}\exp(-bB^2)\right.$$

$$\left.+\frac{1}{m_i^*}\frac{(\mu_{io}^2B^2-\omega^2\tau_i^2-1)\omega^2\tau_i^2}{(1+\mu_{io}^2B^2-\omega^2\tau_i^2)^2+4\omega^2\tau_i^2}[1-\exp(-bB^2)]\right). \tag{25}$$

It is quite instructive to investigate the functional dependence of σ and ϵ_r in the presence of a small magnetic field; this investigation will prove useful when comparing the theory to the experiment. From Eq. (21) and for a concentration of 5×10^{13} cm^{-3} at 77 °K, it is seen that for a magnetic field less than 1.5 kG essentially all the carriers are in the conduction band. This factor, added to the fact that the carrier mobility in the impurity band is much less than that in the conduction band, will cause the contribution of the carriers in the impurity band to the conductivity and the change in the dielectric constant to be negligible. Therefore for small values of the magnetic field σ and ϵ_r are approximately given by

$$\sigma = qN_I\mu_{co}\left(\frac{1+\mu_{co}^2B^2+\omega^2\tau_0^2}{(1+\mu_{co}^2B^2-\omega^2\tau_c^2)^2+4\omega^2\tau^2}\exp(-bB^2)\right) \tag{26}$$

and

$$\epsilon_r=\epsilon_l+\frac{qN_I}{\omega^2\kappa_0 m_c^*}\left(\frac{(\mu_{co}^2B^2-\omega^2\tau_e^2-1)\omega^2\tau_c^2}{(1+\mu_{co}^2B^2-\omega^2\tau_c^2)^2+4\omega^2\tau_c^2}\exp(-bB^2)\right). \tag{27}$$

Differentiating Eq. (26) with respect to B^2 and equating the results to zero gives

$$ay^2+[1+a(3-z)]y^2+[2(1+z)+a(3+2z-z^2)]y$$
$$+[1-2z-3z^2+a(1+3z+3z^2+z^3)]=0, \tag{28}$$

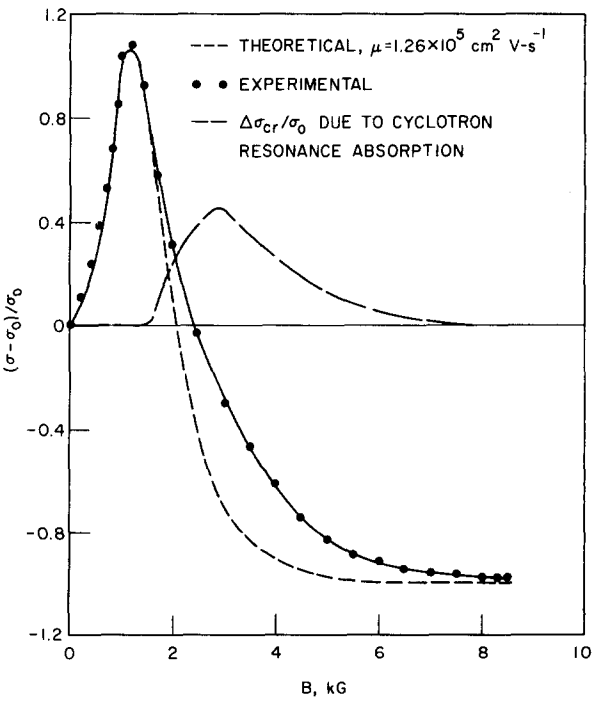

FIG. 4. Comparison of the theoretical and experimental results of $(\sigma-\sigma_0)/\sigma_0$ at 77°K [B is parallel to the (110)-crystal plane].

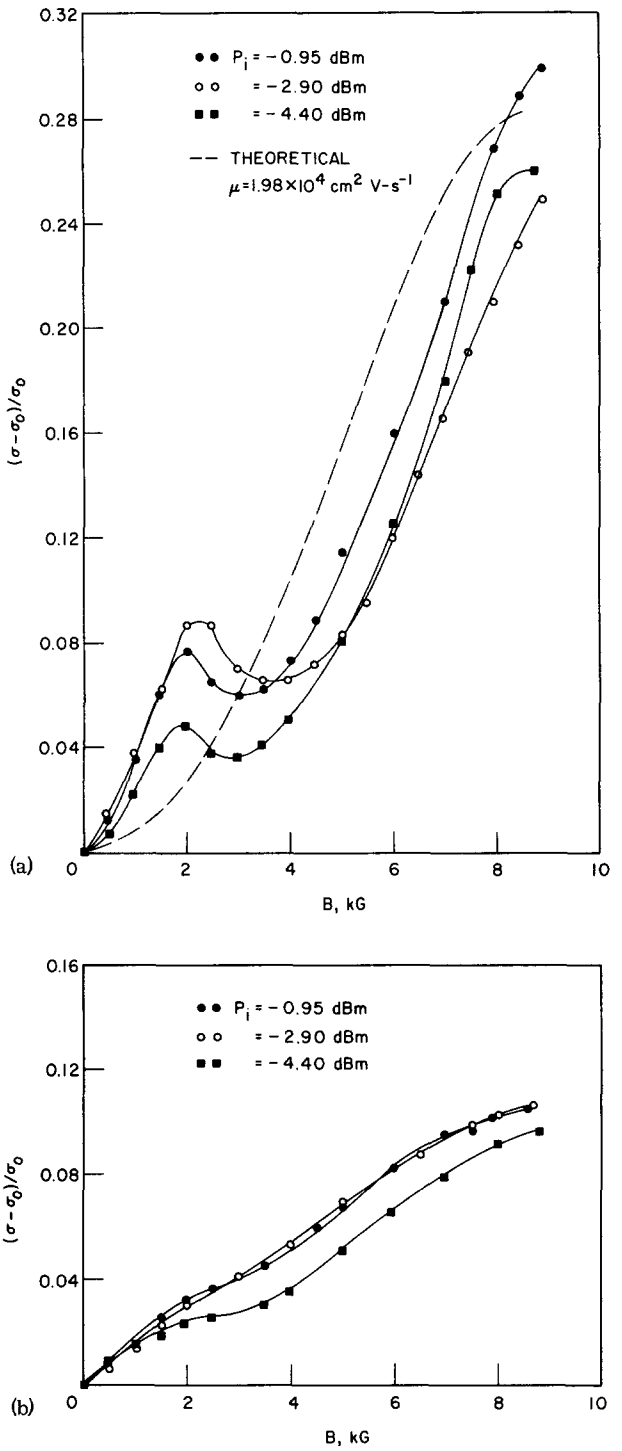

FIG. 5. $(\sigma-\sigma_0)/\sigma_0$ vs B at 175°K. (a) B is parallel to the (110)-crystal plane. (b) B is normal to the (110)-crystal plane.

where $a=b/\mu_{c0}^2$, $y=\mu_{c0}^2B^2$, and $z=\omega^2\tau_c^2$. If a real positive root exists for Eq. (28), the σ-B characteristic will have a critical point at some value of the magnetic field B_0. To investigate this case further it is worth noting that, for most materials of interest (samples with high mobilities) and values of magnetic fields below 1.5 kG, both a and ay are small compared to unity. This reduces Eq. (28) to the following form:

$$y^2+2(1+z)y+(1-2z-3z^2)=0, \tag{29}$$

which gives the following values of y:

$$y=-(1+z)\pm 2[z(1+z)]^{1/2}. \tag{30}$$

Since y is a positive semidefinite quantity, the solution with the negative sign is physically insignificant. Therefore

$$y=-(1+z)+2[z(1+z)]^{1/2}, \tag{31}$$

and the σ-B characteristic has a critical point for a real value of B, if $y>0$ which implies

$$\omega\tau_c\geq 1/\sqrt{3}. \tag{32}$$

The second derivative of σ with respect to y was investigated and turned out to be negative irrespective of the value of z. This shows that if the condition defined by Eq. (32) is fulfilled, σ will assume a maximum. The value of the magnetic field B_0 at which the maximum value of σ occurs is given by

$$B_0=(1/\mu_{c0})\{2\omega\tau_c[1+\omega^2\tau_c^2]^{1/2}-(1+\omega^2\tau_c^2)\}^{1/2}. \tag{33}$$

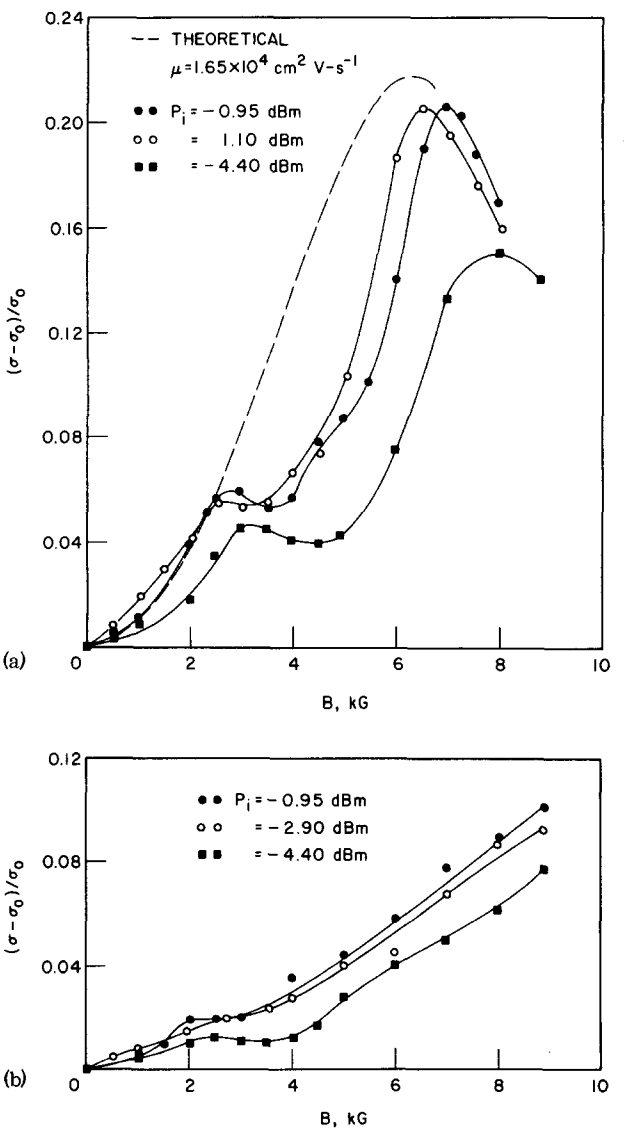

FIG. 6. $(\sigma-\sigma_0)/\sigma_0$ vs B at 200°K. (a) B is parallel to the (110)-crystal plane. (b) B is normal to the (110)-crystal plane.

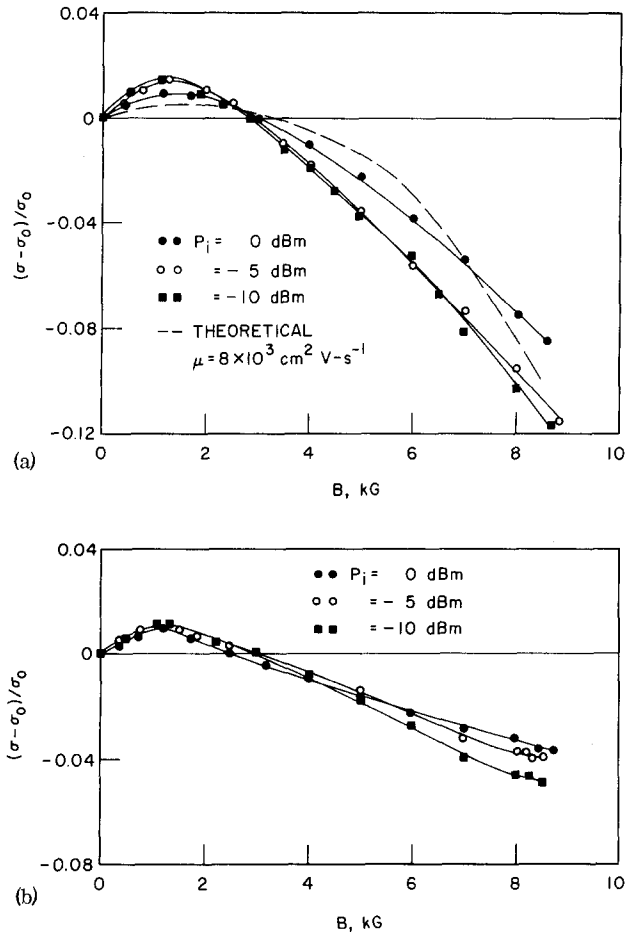

FIG. 7. $(\sigma-\sigma_0)/\sigma_0$ vs B at 295°K. (a) B is parallel to the (110)-crystal plane. (b) B is normal to the (110)-crystal plane.

Solving Eq. (28) for z yields

$$\omega^2\tau_c^2=\tfrac{1}{3}\{(\mu_{c0}^2B_0^2-1)+[2(\mu_{c0}^2B_0^2-1)^2+4\mu_{c0}^2B_0^2]^{1/2}\}. \quad (34)$$

The solution with the negative sign was disregarded as being physically insignificant.

Equation (34) expresses the carrier relaxation time τ_c as a function of the dc mobility μ_{c0} and the magnetic field B_0. This suggests an indirect means for the measurement of the carrier relaxation time if the frequency of the monitoring microwave signal is chosen to satisfy Eq. (32).

EXPERIMENTAL INVESTIGATION

The dependence of the material conductivity and dielectric constant on the microwave power level and the magnetic field intensity was measured as a function of temperature to verify the previous analysis. The high-purity n-type InSb test samples were cut from lapped slices using a wire saw and a slurry consisting of equal weights of glycerine and 240 mesh silicon carbide abrasive. Five-mil wire and light pressure were used, and the samples were cleaned using chemically pure grade benzene. To provide protection for the samples, the unused ones were kept in a container filled with paraffin oil. The sample had dimensions of $1\times2\times4$ mm and the manufacturer (Cominco American, Inc.) supplied the data shown in Table I.

The measurement was carried out using a modification on the cavity perturbation method. The procedure together with the method of analyzing the results has been presented elsewhere.[21] Knowing the cavity coupling factor prior to perturbing the sample together with the change in the reflected power and resonant frequency shift is adequate for studying the conductivity and dielectric constant of the sample. Figure 2(a) shows a schematic diagram of the measurement setup.

The sample was placed under the central post of the reentrant-type cavity system as shown in Fig. 2(b). The cavity system was sealed in vacuum in order to overcome the problems arising from liquid-nitrogen cooling and eliminate the effect of humidity on the resonant frequency shift and the change in the coupling-factor measurements. The cavity setup with the vacuum-tight jacket was placed in a stainless-steel Dewar mounted between the pole pieces of an electromagnet. Thermal contact between the liquid-nitrogen bath and the cavity was achieved by filling the space between the cavity walls and the vacuum jacket with copper powder. A copper-constantan thermocouple was used to monitor the temperature of the sample. Intermediate temperatures between liquid-nitrogen and room temperature were provided by contacting the cavity to a large copper block which acts as a thermal inertia and monitors the temperature of the evacuated cavity system as it warms up very slowly to room temperature. Corrections were made to compensate for the shift in resonant frequency and coupling factor as a result of the temperature change. The test signal was supplied by an ultrastable oscillator which was stabilized at the cavity resonant frequency of 9.675 GHz, and the signal level was varied between −2 and −11 dBm. The experiments were carried out at temperatures of 4.2, 77, 170, 200, and 300°K. In each case the change of the detected power was monitored as the magnetic field was varied between zero and 8.8 kG.

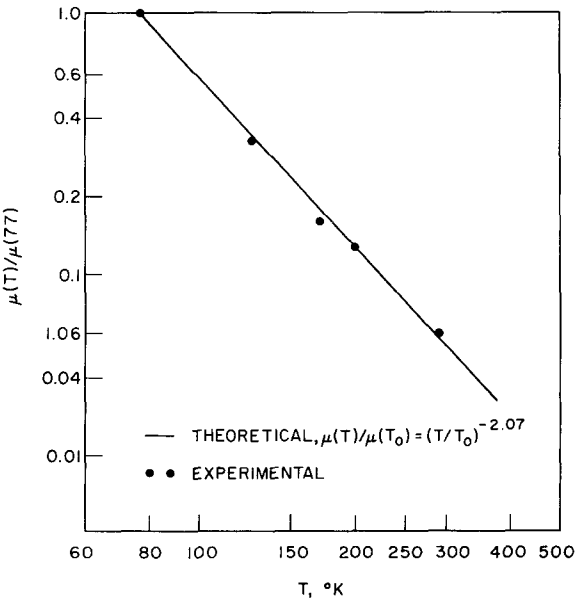

FIG. 8. Temperature dependence of the mobility in InSb.

TABLE I. Data supplied by the manufacturer for the InSb samples at 77 °K.

Resistivity	0.26 to 0.28 Ω cm
Hall mobility	6.1 to 6.2 $\times 10^5$ cm^2 V sec^{-1}
Net carrier concentration	$\sim 4 \times 10^{13}$ cm^{-3}

Behavior of conductivity at liquid-nitrogen temperature

Figure 3 displays the relative change (relative to σ at $B=0$) in the conductivity of the InSb sample as a function of the magnetic field and the microwave signal level measured at 77 °K for different orientations of the magnetic field with respect to the (110)-crystal axis. The curve in Fig. 3(a) indicates a cyclotron resonance absorption whose peak occurs at a magnetic field B_c of approximately 2.9 kG. Assuming the material to be compensated, this resonance could be due to carriers in the impurity, valence, or conduction bands. The effective mass corresponding to this peak can be obtained by equating the cyclotron resonant frequency to the frequency of the incident radiation, i.e.,

$$\omega = (q/m)B_c, \tag{35}$$

where ω is the angular frequency of the incident radiation. Substituting the values of ω, q, and B_c gives a value for m which equals 0.78 times the electronic rest mass. The effective mass of the electrons at the edge of the conduction band was determined earlier and was confirmed recently[22,23] as having a value of $0.0139m_0$. On the other hand, the effective mass of the holes in InSb was shown[24,25] to be $0.4m_0$. This leads to the conclusion that the resonance is due to carriers in the impurity band. Therefore m_i^*, the effective mass of the carriers in the impurity band, equals $0.78m_0$. The ratio of the effective mass in the impurity band to that in the conduction band at liquid-nitrogen temperature is therefore approximately equal to 58.8. The scattering mechanisms for this temperature and above are dominated by either acoustic or polar modes which lead to a mobility proportional to $(m^*)^{-5/2}$ in the first case and $(m^*)^{-3/2}$ in the latter case. Therefore the contribution of the carriers in the impurity band to the conductivity will be neglected.

Since the figures exhibit peaks at a magnetic field B_0 whose value is 1.25 kG, Eq. (33) can be used in conjunction with Eq. (26) to compare the experimental and theoretical results. The relative change in the conductivity was used as the basis for this comparison and is given by

$$\frac{\sigma - \sigma_0}{\sigma_0} = \frac{(1+\mu_{c0}^2 B^2 + \omega^2\tau_c^2)(1+\omega^2\tau_c^2)}{(1+\mu_{c0}^2 B^2 - \omega^2\tau_c^2) + 4\omega^2\tau_c^2} \exp(-bB^2) - 1. \tag{36}$$

The mobility is related to the magnetic field B_0 and $\omega\tau_c$ by Eq. (33) and can be written as

$$\mu_{c_0} = (1/B_0)[2\omega\tau_c(1+\omega^2\tau_c^2)^{1/2} - (1+\omega^2\tau_c^2)]^{1/2}. \tag{37}$$

The net carrier concentration N_I was determined by carrying out a set of Hall measurements on the sample which gave a value of 5×10^{13} cm^{-3}, which is in good agreement with the data supplied by the manufacturer. This value was substituted in Eq. (23) to determine the value of b. Equations (36) and (37) were numerically programmed using the determined values of B_0 and b and taking $\omega\tau_c$ as a variable parameter until the best fit to the experimental results was obtained. Figure 4 shows a comparison between the theoretical and experimental results. It should be emphasized that in deriving Eq. (36), a continuum of states has been assumed for both the impurity and conduction bands. In addition, the energy hf_{c0} associated with the microwave signal has been neglected with respect to the thermal energy. In other words, the cyclotron resonance phenomenon has not been taken into consideration in the theoretical analysis. This accounts for the deviation of the experimental results from the theoretical ones for magnetic fields between 2 and 4.5 kG. The contribution of the resonance absorption to the relative change in the conductivity $\Delta\sigma_{cr}/\sigma_0$ can be obtained from the difference between the experimental and theoretical results. It is included in Fig. 4 for the case where B is parallel to the (110)-crystal plane. It shows a peak at 2.9 kG which is in agreement with the results obtained earlier for the other orientation of the magnetic field.

The value of the magnetic field B_{Fh} at which 90% of the carriers are in the impurity band was found to be 5.75 kG. This value compares very favorably with the theoretical value of 6.5 kG. Figure 3 also shows that the relative change of the material conductivity at liquid-nitrogen and higher temperatures is independent of the incident power level. This indicates that the mobility of the free carriers is independent of the electric field intensity within the sample. Therefore, the free-carrier absorption contribution to the conductivity change is negligible for this temperature range.

Results at temperatures above liquid nitrogen

The experimental procedure is the same at all temperatures except at room temperature. At this temperature the change in the detected voltage as a result of changing the magnetic field is very small and, in order to improve the accuracy of the measurements, the change in the detected signal was amplified using a differential amplifier. In comparing the experimental and theoretical results the value of the intrinsic concentration was used in place of N_I in Eq. (36), since the material is essentially intrinsic at these temperatures and the hole mobility is much smaller than the electron mobility. Table II shows the intrinsic carrier concentration of InSb at the temperatures of interest. It is clear from Table II that the intrinsic concentration above 175 °K is much higher than the net carrier concentration measured at 77 °K (5×10^{13} cm^{-3}). Moreover the values cited in Table II agree with those obtained by Hall measurements at 290 °K.

Figures 5–7 show the experimental results for the

TABLE II. Intrinsic carrier concentration in InSb.

Temperature (° K)	Intrinsic concentration (cm^{-3})
77	2.5×10^9
175	3.5×10^{14}
200	1.13×10^{15}
295	2.15×10^{16}

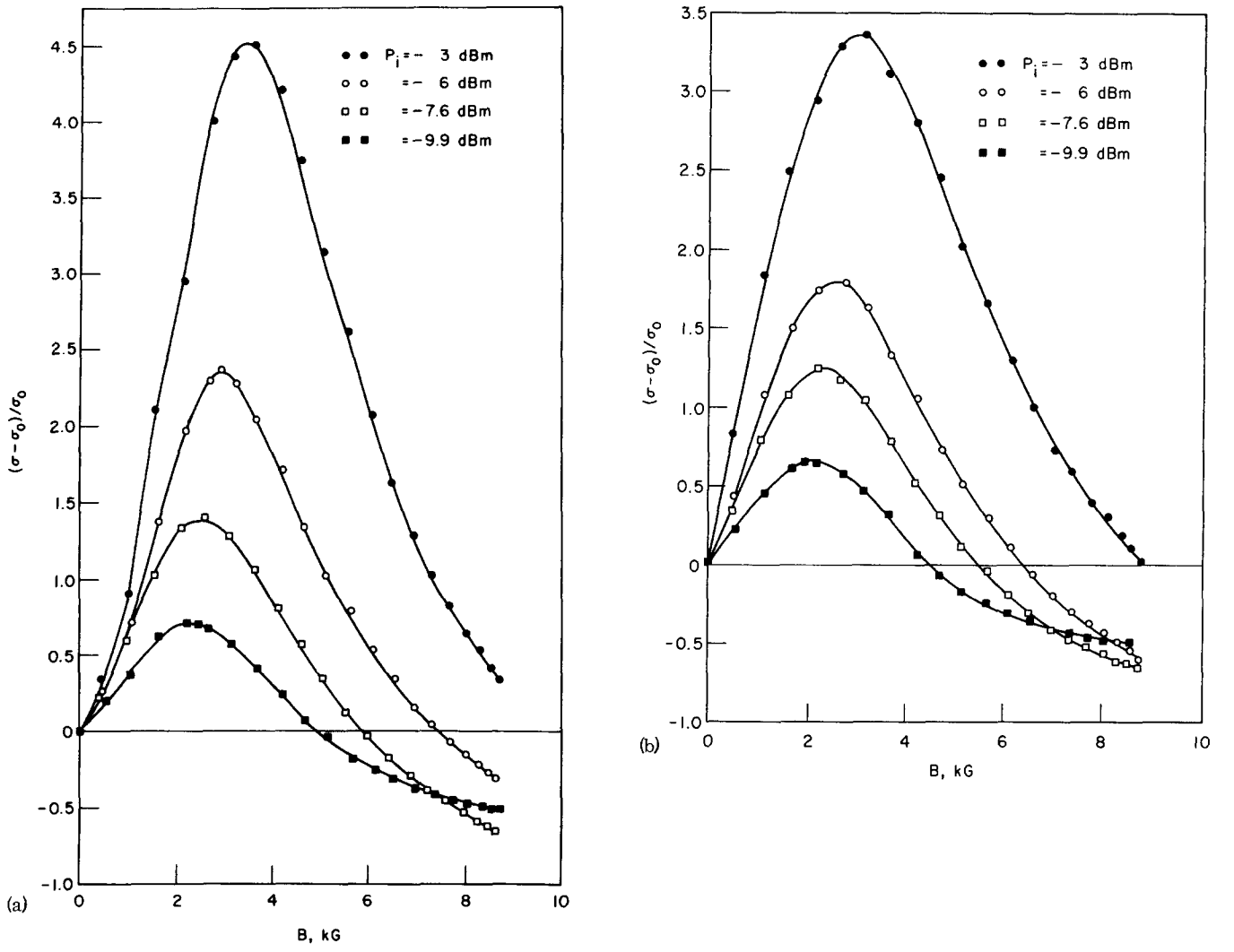

FIG. 9. $(\sigma-\sigma_0)/\sigma_0$ vs B at 4.2°K. (a) B is parallel to the (110)-crystal plane. (b) B is normal to the (110)-crystal plane.

relative change in the conductivity versus magnetic field. The theoretical results are included in the figures for the cases where B is parallel to the (110)-crystal axis since they are characterized with the minimum values for the cyclotron resonance absorption. The main conclusions from these figures are

(i) The magnitude of the relative change in conductivity decreases as the temperature is increased and is much smaller than that at liquid-nitrogen temperature. This is due to the fact that the mobility decreases with temperature.

(ii) The freeze-out effect has not been observed at 175, 200, and 290 °K for magnetic fields as high as 8.8 kG; this is to be expected since the theoretical values of B_{Fh} are approximately 19, 30, and 41 kG at 175, 200, and 295 °K, respectively.

(iii) The peak of the absorption occurs at about 3 kG for both measurements at 175 and 200 °K which indicates that m_i^* is independent of the temperature.

A plot of the measured values of mobility (normalized to the value at liquid-nitrogen temperature) versus the temperature is shown in Fig. 8. The dependence of the mobility on temperature can be represented by the expression

$$\mu = \mu_1 T^{-2.07}, \tag{38}$$

where μ_1 is the mobility at 77 °K and has a value of 1.26×10^5 cm^{2}Vsec^{-1}. This indicates that the scattering mechanism is a combination of acoustic and polar lattice scattering. The lower value of the mobility at 77 °K is obviously due to the fact that the sample is compensated.

Behavior of conductivity at liquid-helium temperature

Figures 9 are plots of the relative change of the conductivity versus magnetic field for several X-band signal levels at 4.2 °K. The figures show a marked dependence of conductivity on the incident power level. The results are in contrast with the behavior at liquid-nitrogen temperature and above, where the conductivity is independent of the signal level. The change in the conductivity is due to free-carrier absorption which gives rise to an increase in the carrier temperature above that of the lattice thermal equilibrium, and in turn will change the carrier mobility. On the other hand, the

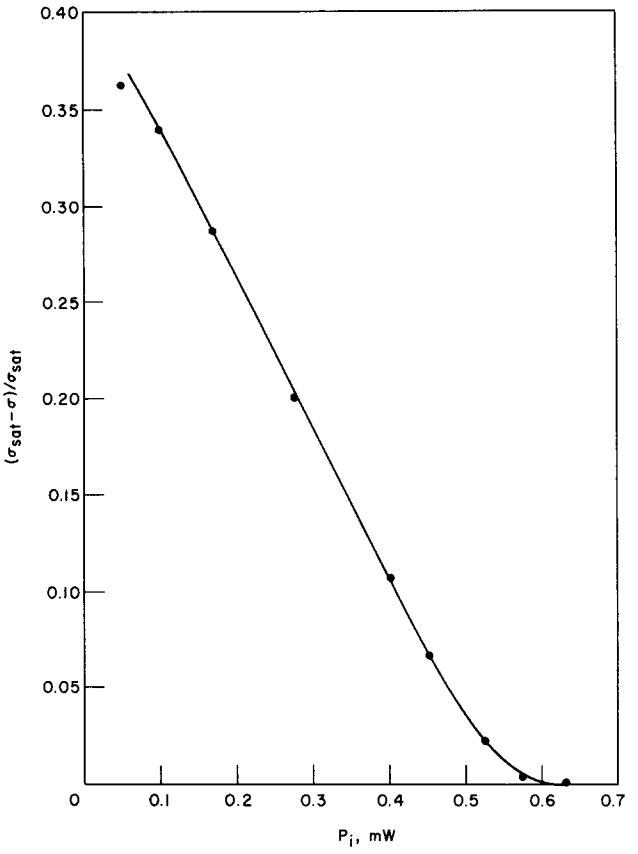

FIG. 10. Dependence of the sample conductivity on the incident power level at 4.2 °K ($B=0$).

change in conductivity is not significant at liquid-nitrogen temperature or above for signal levels of below 1 mW. This means that the hot-electron effect in InSb is very pronounced at liquid-helium temperature. The results of measuring the dependence of the conductivity on the incident power level are presented in Fig. 10. The conductivity saturates for power levels above −2 dBm and exhibits a linear dependence on the incident power for signal levels below −3 dBm. The hot-electron effect in InSb due to steady electric field (dc) was discussed by several authors, among them are Kogan[23] and Putley,[13] where it was shown that for small steady electric fields the conductivity varies quadratically with the electric field intensity. This agrees favorably with the results for the microwave field presented in Fig. 10, since the square of the electric field intensity under the central post is proportional to the incident power.

A knowledge of the effective carrier temperature is necessary to compare the theoretical and experimental results. The effective temperature can be determined by studying the temperature dependence of the mobility as a function of temperature at approximately 4.2 °K which could not be achieved with the available experimental facilities.

Results of study of relative dielectric constant

The dependence of the material dielectric constant on electric and magnetic fields was investigated at temperatures between 4.2 and 290 °K. Measurement of the cavity filling factor and resonant frequency shift is adequate for this purpose.[21] The circuit shown in Fig. 2(a) was used to measure the cavity resonant frequency shift as a result of perturbing the sample. On the other hand, the cavity filling factor was measured in a separate experiment and was found to have a value of 0.006. Measurements were carried out for two cases. In the first case the material dielectric constant was investigated as a function of the temperature for different signal levels at zero magnetic field. The cavity resonant frequency shift arises from two effects, namely, the change in the material parameters and the thermal expansion of the cavity walls. The experimentally measured values for the resonant frequency shift as a result of varying the sample temperature between 77 and 290 °K are shown in Fig. 11. A plot of the theoretical values of the resonant frequency shift for the empty cavity is also included. It is seen from this figure that the net frequency shift due to variation of the sample temperature between 77 and 290 °K is essentially zero. Therefore the material dielectric constant is independent of the temperature over the range of 77 to 290 °K. Moreover the dielectric constant was found to be independent of the X-band signal level over the same temperature range. This shows that between 77 and 290 °K, all charge carriers are in the conduction band in the absence of a magnetic field. This is in agreement with the discussion presented earlier.

The second set of measurements deals with the dependence of ϵ_r on magnetic field. Experiments were carried out for temperatures between 4.2 and 290 °K. The resonant frequency shift at 175 °K and above was found to be of the same order as the experimental uncertainties

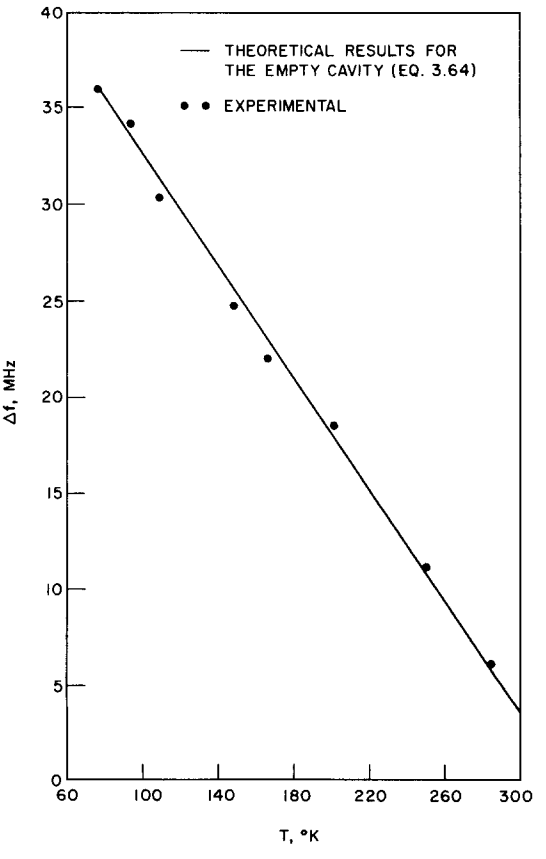

FIG. 11. Cavity resonant frequency shift vs T ($B=0$).

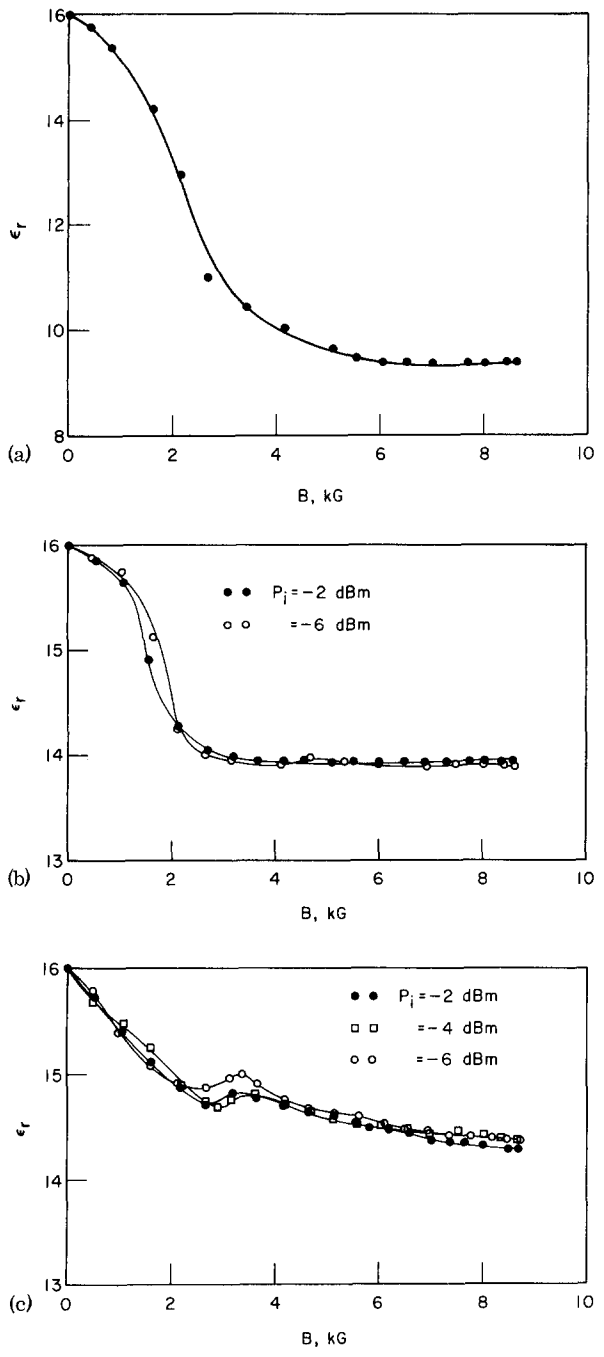

FIG. 12. Dielectric constant vs B.(a) at 4.2 °K, B is parallel to the (110)-crystal plane; (b) at 77 °K, B is parallel to the (110)-crystal plane; (c) at 77 °K, B is normal to the (110)-crystal plane.

(10 kHz when using a spectrum analyzer). These results will not be presented here. Figure 12(a) shows the experimental results of the dielectric constant of the sample at 4.2 °K. On the other hand, Figs. 12(b) and 12(c) show similar results at 77 °K for different orientations of the magnetic field with respect to the (110)-crystal plane. The figures exhibit the same resonance absorption effects as those for the conductivity presented in the earlier sections.

CONCLUSIONS

A thorough evaluation of the microwave properties of bulk n-type InSb in the presence of a dc magnetic field has been conducted. A two-band conduction model was assumed for this purpose. In the analysis a hydrogenic model was utilized; the impurity ions were assumed to be arranged on a uniform lattice and the carriers were assumed to have a Maxwellian distribution. An expression for the magnetic field required to freeze out the carriers in the impurity band was derived. Cavity perturbation techniques using an equivalent circuit approach were utilized to compare the theoretical and experimental results. The method was found to be very sensitive and highly versatile. It eliminates the need for contacting the sample and makes it possible to utilize low signal levels to avoid electron heating. The theory and experiment were found to be in good agreement, which justifies the equivalent circuit approach.

The conductivity of InSb proved to be independent of the microwave signal level below 1 mW for temperatures above 77 °K. This shows that the hot-electron effect is negligible over this temperature range. In addition, the scattering mechanism was found to be dominated by acoustic and optical modes above 77 °K. However, the hot-electron effect was found to be pronounced at liquid-helium temperature. The conductivity varies linearly with the signal level for signals below −3 dBm and saturates at signals above −2 dBm. The concept of electron temperature can be utilized to explain the saturation phenomena. Since at 4.2 °K the scattering mechanism is dominated by ionized impurity scattering, the electron temperature will increase above that of the lattice if $\tau_c \gg \tau_{ee}$, where τ_c is the energy relaxation time and τ_{ee} is the effective time of the electron-electron collision redistributing the energy among the system of electrons. The increase in the carrier temperature results in a corresponding increase in mobility. Studies made on the dependence of τ_c on temperature by Whalen and Westgate[26] show that τ_c is essentially independent of temperature up to about 14 °K, and above that temperature τ_c decreases considerably with increasing temperature. Therefore, as the incident microwave signal level increases, the electron temperature will increase above 4.2 °K until it reaches a value of approximately 14 °K where the optical phonon scattering becomes appreciable. As a result τ_c starts to decrease causing the carrier temperature to increase at a lower rate. Finally, as the inequality $\tau_c \gg \tau_{ee}$ becomes invalid, the carrier temperature saturates and the material conductivity becomes independent of the microwave power level.

*Work supported by the National Aeronautics and Space Administration under Grant No. NGL 23-005-183.

†Present address: Bell Telephone Laboratories, Holmdel, N.J.

[1]L. B. Kreuzer and C. K. N. Patel, Science **173**, 45 (1971).
[2]I. I. Eldumiati and G. I. Haddad, IEEE Trans. Electron Devices (to be published).
[3]J. J. Whalen and C. R. Westgate, in *The Symposium on Submillimeter Waves, Brooklyn, New York, 1970* (Polytechnic Press, Brooklyn, N.Y., 1971).
[4]R. W. Keyes and R. J. Sladek, J. Phys. Chem. Solids **1**, 143 (1956).
[5]J. R. Apel, T. O. Poehler, and C. R. Westgate, Appl. Phys. Lett. **14**, 161 (1969).
[6]R. J. Sladek, Phys. Rev. **105**, 460 (1957).
[7]E. H. Putley, J. Phys. Chem. Solids **22**, 241 (1961).
[8]V. A. Danilychev and P. N. Lebedev, JETP Lett. **2**, 300 (1965).

[9]E. M. Conwell, Phys. Rev. **103,** 51 (1956).
[10]C. S. Hung, Phys. Rev. **79,** 727 (1950).
[11]Y. Yafet, R. W. Keyes, and E. N. Adams, J. Phys. Chem. Solids **1,** 137 (1956).
[12]M. A. C. S. Brown and M. F. Kimmit, Infrared Phys. **5,** 93 (1965).
[13]E. H. Putley, *Semiconductors and Semimetals*, edited by A. C. Beer and R. K. Willardson (Academic, New York, 1966), Vol. 1.
[14]C. H. L. Goodman, Nature (Lond.) **187,** 590 (1960).
[15]E. Mooser and W. B. Pearson, Nature (Lond.) **190,** 406 (1961).
[16]W. Cochran, Nature (Lond.) **191,** 60 (1961).
[17]M. Hass and B. W. Henvis, J. Phys. Chem. Solids **23,** 1099 (1962).
[18]M. Born and K. Huang, *Dynamical Theory of Crystal Lattices* (Oxford U. P., London, 1954).
[19]A. E. Attard and L. V. Azaroff, J. Appl. Phys. **34,** 774 (1963).
[20]In obtaining this value of ν_0, all the carriers are assumed to be in the conduction band in the absence of a magnetic field.
[21]I. I. Eldumiati and G. I. Haddad, IEEE Trans. Microwave Theory Tech. **20,** 126 (1972).
[22]E. J. Johnson and D. H. Dickey, Phys. Rev. **1,** 2676 (1970).
[23]Sh. M. Kogan, Sov. Phys.-Solid State **4,** 1386 (1963).
[24]F. Stern in *Preceedings of the International Conference on Semiconductor Physics, Prague, Czechoslovakia, 1961* (Academic, New York, 1961), p. 363.
[25]D. M. Bagguley, M. L. Robinson, and R. A. Strabling, Phys. Lett. **6,** 143 (1963).
[26]J. J. Whalen and C. R. Westgate, Appl. Phys. Lett. **15,** 292 (1969).